MCB
Journals.ASM.org

PLEKHG2 Promotes Heterotrimeric G Protein βγ-Stimulated Lymphocyte Migration via Rac and Cdc42 Activation and Actin Polymerization

Caitlin Runne,[a] Songhai Chen[a,b]

Departments of Pharmacology[a] and Internal Medicine,[b] Roy J. and Lucille A. Carver College of Medicine, Holden Comprehensive Cancer Center, University of Iowa, Iowa City, Iowa

PLEKHG2 is a Dbl family Rho guanine nucleotide exchange factor (RhoGEF) whose gene was originally identified as being upregulated in a leukemia mouse model and was later shown to be activated by heterotrimeric G protein βγ (Gβγ) subunits. However, its function and activation mechanisms remain elusive. Here we show that, compared to its expression in primary human T cells, its expression is upregulated in several leukemia cell lines, including Jurkat T cells. Downregulation of PLEKHG2 in Jurkat T cells by small interfering RNAs (siRNAs) specifically inhibited Gβγ-stimulated Rac and Cdc42, but not RhoA, activation. Consequently, suppressing PLEKHG2 expression blocked actin polymerization and SDF1α-stimulated lymphocyte migration. Additional studies indicate that Gβγ likely activates PLEKHG2, in part by binding the N terminus of PLEKHG2 to release an autoinhibition imposed by its C terminus, which interacts with a region encompassing the catalytic Dbl homology (DH) domain. As a result, overexpressing either the N terminus or the C terminus of PLEKHG2 blocked Gβγ-stimulated Rac and Cdc42 activation and prevented Jurkat T cells from forming membrane protrusions and migrating. Together, our studies have provided the first evidence for the endogenous function of PLEKHG2, which may serve as a key Gβγ-stimulated RhoGEF that regulates lymphocyte chemotaxis via Rac and Cdc42 activation and actin polymerization.

Rho GTPases are a subfamily of Ras superfamily proteins. Approximately 25 Rho GTPases have been identified, of which Rac, Cdc42, and RhoA are the best characterized (1). Rho GTPases regulate many aspects of cellular functions, including actin cytoskeletal organization, cell cycle progression, gene transcription, and cell migration (2, 3). Aberrant activation of Rho GTPases has been implicated in many diseases, including the initiation and progression of leukemia and lymphoma (4). Rho GTPases are activated by Rho guanine nucleotide exchange factors (RhoGEFs), which mediate the switch from an inactive GDP-bound form to an active GTP-bound form. There are a remarkably large number (~100) of RhoGEFs, a majority of which (~70) belong to the Dbl family (2, 5). Dbl RhoGEFs are characterized by the presence of a catalytic Dbl homology (DH) domain followed by a pleckstrin homology (PH) domain. The activity of RhoGEFs is often regulated by cell surface receptors, such as growth factor receptors and G protein-coupled receptors (GPCRs). GPCRs may regulate the activity of RhoGEFs either through direct interaction of activated heterotrimeric G proteins with a RhoGEF or through downstream effectors of G proteins, such as kinases (6). With some exceptions, the function and activation mechanisms of many RhoGEFs remain largely unknown.

PLEKHG2 is a Dbl family RhoGEF that was originally identified by its upregulation by proviral integration at *Evi24*, a common site of retroviral integration in AKXD B cell and BXH-2 myeloid leukemia and lymphoma (7). *In vitro* assays using the purified DH-PH domain of PLEKHG2 revealed that PLEKHG2 specifically activated Cdc42 but not Rac1 and RhoA. Moreover, overexpression of the full-length or C-terminally truncated form of PLEKHG2 caused morphological transformation of NIH 3T3 cells, suggesting that its upregulation may contribute to leukemogenesis (7). However, formal proof of the function of PLEKHG2 in leukemogenesis is still lacking. In a recent screen for RhoGEFs regulated by the heterotrimeric G proteins, PLEKHG2 was shown to be specifically activated by G protein βγ (Gβγ) subunits but not Gα subunits (8). Stimulation of PLEKHG2 by Gβγ induced serum response element (SRE)-mediated gene transcription via activation of Rac and Cdc42 but not RhoA. Gβγ was found to interact with the N-terminal region of PLEKHG2, and this interaction was postulated to release an autoinhibition imposed by the C terminus, resulting in activation (8). However, direct evidence to support this mechanism of PLEKHG2 activation is still lacking. Moreover, the role of endogenous PLEKHG2 in cellular functions remains unknown.

It is well established that heterotrimeric G protein βγ subunits play a critical role in mediating leukocyte chemotaxis during immune surveillance and response to various insults (9, 10). Following chemoattractant binding to GPCRs, Gβγ is activated by release from Gi/o proteins (11, 12). Activated Gβγ transmits chemotactic signals by stimulating Rho GTPases to facilitate actin cytoskeleton organization for leukocyte polarization and migration (1). Several RhoGEFs, including phosphatidylinositol (3,4,5)-trisphosphate (PIP_3)-dependent Rac exchanger 1 (pRex1), PIXα, dedicator of cytokinesis 2 (DOCK2), and ARHGEF5, have been shown to be activated downstream of

Received 10 July 2013 Returned for modification 14 August 2013
Accepted 23 August 2013
Published ahead of print 3 September 2013
Address correspondence to Songhai Chen, songhai-chen@uiowa.edu.
Supplemental material for this article may be found at http://dx.doi.org/10.1128/MCB.00879-13.

doi:10.1128/MCB.00879-13

Gβγ, either by direct interaction with Gβγ or by other Gβγ-stimulated signaling molecules, such as p21-activated kinase 1 (PAK1) and phospholipase D (PLD), to facilitate Rac, Cdc42, or RhoA activation for leukocyte migration (13–18). It is not clear if PLEKHG2 also plays a role in Gβγ-mediated Rho GTPase activation and leukocyte migration.

In this study, we have evaluated the role of endogenous PLEKHG2 in mediating Gβγ-induced lymphocyte migration and the mechanism of its activation by Gβγ. We show that PLEKHG2 is upregulated in several leukemia cell lines and that it specifically mediates Gβγ-stimulated Rac and Cdc42 activation to facilitate actin polymerization and lymphocyte migration. Moreover, we demonstrate that PLEKHG2 is autoinhibited by the binding of its C-terminal domain to the N-terminal region containing the DH and PH domains and that Gβγ likely activates PLEKHG2, at least in part, by binding to its N terminus to release autoinhibition. Together, our results have demonstrated that endogenous PLEKHG2 functions as a novel Gβγ-stimulated RhoGEF, which may mediate chemokine-induced chemotaxis of lymphocytes overexpressing PLEKHG2.

MATERIALS AND METHODS

Reagents. Human SDF1α was obtained from PeproTech. Pertussis toxin (PTx), mouse anti-FLAG (M2), and FLAG (M2) magnetic beads were from Sigma. Rabbit anti-AKT, mouse anti-phospho-AKT473, rabbit anti-extracellular signal-regulated kinase 1 and 2 (anti-ERK1/2), and mouse anti-phospho-ERK1/2 were from Cell Signaling Technology, Inc. Rabbit anti-PLEKHG2 and WDR26 were from Bethyl Laboratories. Rabbit anti-Gβ, rabbit anti-Cdc42, and mouse anti-RhoA were obtained from Santa Cruz Biotechnology. Mouse anti-Rac antibody was obtained from EMD Millipore. Mouse antimortalin was obtained from the University of California—Davis/NIH NeuroMab facility. Streptavidin-conjugated magnetic beads were obtained from Pierce. OKT3 was purified from the supernatant of the hybridoma culture (19). All other materials were obtained with the highest quality available.

Cell culture. HEK293A and HEK293FT cells (Life Technologies) were grown in Dulbecco's modified Eagle's medium (DMEM) (Life Technologies) supplemented with 10% fetal bovine serum (FBS) at 37°C and 5% CO_2. Jurkat T cells (ATCC), HL60 cells (ATTC), and the B lymphocyte cell lines GM19116C and GM18500B (Coriell Cell Repositories) were grown in RPMI medium supplemented with 10% FBS and 10 mM HEPES. Differentiation of HL60 cells to human neutrophil-like cells was induced by the addition of 1.3% dimethyl sulfoxide (DMSO) for 5 to 7 days (19).

Plasmid constructs and small interfering RNAs (siRNAs). The cDNAs for human PLEKHG2 and all PLEKHG2 truncation mutants were generated by PCR. Constructs were prepared using the Gateway system, cloning DNA first into the entry vector pENTR/D-TOPO and then into the destination vector pcDNA3.1-DEST-FLAG, pcDNA3.1-DEST-myc, pCS2-mCherry-DEST, or pcDNA3.1-SBP-FLAG-DEST. The resulting destination vectors each contain the DNA sequences for the epitope tag FLAG, streptavidin-binding peptide (SBP) and FLAG, myc, or mCherry at the 5′ end of the inserted gene.

The plasmid pCIN3×FLAG-tagged Gβ1 point mutants were kindly provided by A. V. Smrcka (University of Rochester Medical Center). pC-HA-Vav1 was purchased from Addgene.

Control siRNA targeting random sequences and PLEKHG2 targeting siRNAs 1 and 2 were obtained from Dharmacon and Life Technologies Corporation, respectively. Their targeting sequences are 5′-GTACCTTC GGCCTAACAGT-3′ (control), 5′-TCGCGAGATGGTGGAGGAAGCT ATT-3′ (PLEKHG2 siRNA 1), and 5′-CCTTTGGACACGTGCTGGTAT GTGA-3′ (PLEKHG2 siRNA 2).

The plasmid pcDNA3 PAK-PBD-YFP, encoding the Rac/Cdc42 binding domain of PAK (PAK-PBD) fused to yellow fluorescent protein (YFP), was a gift from Jingsong Xu (University of Illinois at Chicago), and pCS2 Lifeact-RFP, encoding the first 17 amino acids of the actin-binding protein 140 probe (Lifeact) fused to red fluorescent protein (RFP), was a gift from Fang Lin (University of Iowa).

Isolation and expansion of human primary T cells. Human primary T cells were isolated from peripheral blood leukocytes recovered from leukocyte depletion filters obtained at the DeGowin Blood Center (University of Iowa Hospitals and Clinics). Briefly, peripheral blood leukocytes were flushed from the leukocyte depletion filters with phosphate-buffered saline (PBS) buffer (pH 7.4) containing 5 mM EDTA (50 ml per filter). Thirty-five milliliters of filter-leukocytes was then overlaid on top of 15 ml of IsoPrep (Axis-Shield PoC AS). After centrifugation at 800 × *g* for 20 min at room temperature (RT), mononuclear leukocytes were recovered from the interphase and used for isolation of untouched human T cells using the Dynal T cell negative isolation kit (Life Technologies). To expand the human T cells, purified T cells were cultured in RPMI media containing 10% fetal calf serum (FCS), 10 ng/ml interleukin 2 (IL-2), and an equal number of Dynabeads CD3/CD28 T cell expander beads (Life Technologies). Forty-eight hours postexpansion, human T cells were harvested for Western blotting of PLEKHG2 expression.

Transfection. Transient transfection of HEK293A cells was achieved using Polyjet DNA *in vitro* transfection reagent (Signagen). Stable expression of FLAG-tagged PLEKHG2 was performed by transfecting HEK293FT cells with constructs expressing PLEKHG2 and selecting with hygromycin (0.5 mg/ml) for 6 weeks.

Transient transfection of Jurkat T cells was performed using the Neon transfection system (Life Technologies) by following the manufacturer's protocol and using parameters described previously (20). GM18500B cells were transiently transfected using the Neon transfection system with 100-μl electroporation tips and the electroporation parameters 1,500 V for 25 ms per pulse (21). Up to 80 to 90% and 90 to 100% transfection efficiency for plasmids and oligonucleotides, respectively, could be obtained, as judged by the percentage of green fluorescent protein (GFP)- or fluorescence-positive cells 1 day after transfection of plasmids carrying enhanced GFP (EGFP)- or fluorescein isothiocyanate (FITC)-labeled oligonucleotides. Cells were harvested for assays 72 h posttransfection.

Coimmunoprecipitation and Western blotting analysis. To coimmunoprecipitate FLAG-PLEKHG2 with endogenous Gβγ, Jurkat T cells transiently transfected with FLAG-PLEKHG2 or HEK293FT cells stably expressing FLAG-PLEKHG2 were serum starved overnight in the presence or absence of PTx (0.2 μg/ml). Cells were stimulated with SDF1α (50 nM) or lysophosphatidic acid (LPA) (10 μM) for 0 to 15 min and lysed with modified radioimmunoprecipitation assay (RIPA) buffer (50 mM Tris-HCl, pH 7.4, 150 mM NaCl, 1% Nonidet P-40, 1 mM EDTA) containing protease inhibitors. FLAG-PLEKHG2 was immunoprecipitated with anti-FLAG M2 magnetic beads. The immunoprecipitates were resolved by SDS-PAGE and analyzed by Western blotting.

Analysis of complex formation between myc-tagged PLEKHG2 truncation mutants and an SBP-FLAG-tagged C-terminal mutant (SBP-FLAG–965-1386) was performed after their expression in HEK293A cells and overnight serum starvation. SBP-FLAG–965-1386 was precipitated with streptavidin-conjugated magnetic beads.

Expression of endogenous PLEKHG2 in leukemia cell lines and in human lymphocyte samples was analyzed using a horseradish peroxidase (HRP)-conjugated anti-rabbit secondary antibody, followed by treatment with enhanced chemiluminescence stain. Blots were exposed on X-ray films and developed using a Kodak imager. All other proteins were resolved by Western blotting using the Odyssey infrared imaging system (LI-COR Biosciences). For analysis of ERK1/2 and AKT phosphorylation in Jurkat T cells, cells were serum starved at least 6 h and stimulated with 50 nM SDF1α.

Flow cytometric analysis of CXCR4 expression. The expression level of CXCR4 in siRNA-treated Jurkat T cells was determined as described previously (20). Briefly, 48 to 62 h posttransfection, cells (5×10^5) were labeled with a control IgG or a phycoerythrin (PE)-conjugated mouse

anti-human CXCR4 antibody (5 μg/ml) (R&D Systems, Inc.) for 45 min at 4°C. After being washed with saline 3 times, cells were analyzed by flow cytometry (BD FACSCalibur).

Chemotaxis assays. Chemotaxis of Jurkat T and GM18500B cells expressing a control siRNA or a siRNA targeting PLEKHG2 and Jurkat T cells expressing mCherry-tagged PLEKHG2 mutant constructs in response to SDF1α was assessed by the Transwell assay using the modified Boyden chamber (Neuro Probe), as described previously (19–21).

Rho GTPase activation assays. The activation of Rac1, RhoA, and Cdc42 in Jurkat T cells was assessed by glutathione *S*-transferase (GST) pulldown assays using a GST fusion protein containing either the Rac1/Cdc42 binding domain of PAK1 (PBD) or the RhoA binding domain of rhotekin (RBD), as described previously (22). GST-PBD and GST-RBD were expressed in *Escherichia coli* BL21 after induction with 0.8 mM IPTG (isopropyl-β-D-thiogalactopyranoside) for 3 h at 37°C. *E. coli* cells were lysed in lysis buffer (50 mM Tris-HCl, pH 7.5, 150 mM NaCl, 5 mM $MgCl_2$, 1 mM dithiothreitol [DTT], 1 mM EDTA) containing protease inhibitors and aliquoted for storage at −80°C. Prior to Rho GTPase activation assays, GST-PBD and GST-RBD were freshly purified by incubation of lysates with glutathione-Sepharose beads for 1 h at 4°C.

To determine Rho GTPase activities, Jurkat T cells were serum starved overnight. Following stimulation with SDF1α (50 nM), cells (1×10^7) were lysed in 0.5 ml of lysis buffer (50 mM Tris-HCl, pH 7.5, 10 mM $MgCl_2$, 200 mM NaCl, 1% Nonidet P-40, 5% glycerol) containing protease and phosphatase inhibitors and then incubated for 1 h with 30 μg of GST-PBD or GST-RBD bound to glutathione-Sepharose beads (19). After a washing with lysis buffer, protein complexes were resolved by SDS-PAGE and detected by Western blotting using the Odyssey infrared imaging system (LI-COR Biosciences).

Actin polymerization assay. SDF1α-stimulated actin polymerization in Jurkat T cells was determined as described previously with modification (23). Briefly, after serum starvation overnight, Jurkat T cells (1×10^6) were stimulated with SDF1α (20 nM) and stopped with fixation buffer (3.7% paraformaldehyde, 0.1% Triton X-100, 20 mM KPO_4, 10 mM PIPES, 5 mM EGTA, 2 mM $MgCl_2$, pH 6.8). After incubation at room temperature for 15 min, cells were centrifuged at 16,000 × *g* for 1 min. The pellets were suspended in 100 μl of PBS containing 10% FCS, 0.1% Triton X-100, and 100 nM Alexa Fluor 488-conjugated phalloidin. After incubation at room temperature for 1 h, the pellets were washed with PBS and then resuspended in 200 μl PBS by sonication. The fluorescence intensity of the pellets was then quantified by using the Synergy 4 microplate reader (BioTek).

Live-cell imaging. To monitor Rac/Cdc42 activation and actin polymerization, Jurkat T cells were transfected with PAK-PBD-YFP and Lifeact-RFP and used for live-cell imaging 24 h posttransfection. To determine the effect of PTx treatment, cells were treated with PTx (0.2 μg/ml) overnight immediately after transfection. To determine the effect of PLEKHG2 knockdown, cells were transfected with a control or PLEKHG2 siRNA. Forty-eight hours posttransfection, cells were retransfected with a control or PLEKHG2 siRNA together with PAK-PBD-YFP and Lifeact-RFP and used for imaging analysis 24 h later. To examine the effect of PLEKHG2 mutants, cells were cotransfected with PAK-PBD-YFP and the mCherry, mCherry–1-135, or mCherry–965-1386 mutant of PLEKHG2 and used for imaging analysis 24 h posttransfection.

Transfected Jurkat T cells were washed with PBS and then incubated in serum-free and phenol red-free DMEM-F12 media for 2 h. Cells were then resuspended in modified Hanks balanced salt solution (HBSS) buffer (20 mM HEPES, pH 7.2, 150 mM NaCl, 4 mM KCl, 1 mM $MgCl_2$, 1.2 mM $CaCl_2$) containing 0.9% glucose and 0.1% human serum albumin and placed in the center of a coverslip in a Chamlide magnetic chamber (LCI). After incubation at 37°C with 5% CO_2 for 10 min, nonadherent cells were removed by a wash with HBSS. Images were acquired at 37°C using a Leica inverted spinning-disk confocal microscope equipped with a temperature-controlled enclosed chamber and an electron-multiplying charge-coupled device (EM-CCD) digital camera (Hamamatsu Photonics) driven by the Metamorph image acquisition and processing software (Molecular Devices). Images were taken every 15 s with a 63×, 1.30-numerical-aperture (NA) oil immersion objective (Leica). Prior to the addition of a uniform concentration of SDF1α (50 nM) or OKT3 (10 μg/ml) to the cells, images were taken for 1 min. After that, continuous real-time frame acquisition was continued for 5 to 10 min.

Image analysis. Images were processed using ImageJ 1.46r (NIH). To correct for position shifts during time-lapse imaging, the position of cells in each image series was first aligned to that of cells in the first frame using the plug-in Stackreg or cvMatch_template. A custom-written macro for ImageJ software was used to autocontrast image series, and the dynamics of PBD-PAK-YFP and Lifeact-RFP was quantified as a motility index (MI). The motility index represents the average difference in position and pixel area of cells between two consecutive frames in a time-lapse series. To calculate MI, we first quantified the nonoverlapping pixel area with counted fluorescence by subtracting two consecutive images pixel by pixel after autocontrasting. The absolute difference in pixel area was then expressed as a fraction of the total pixel area in the two consecutive frames. The overall cellular motility index was calculated by averaging the frame-by-frame motility indexes. The motility index varies from 0 to 1, with 0 indicating no movement and change in pixel area and 1 indicating a complete change in position of the cell. Thus, to calculate the MI of the first two frames, we used the equation $MI_{(1,2)}$ = mean{subtract[difference(frame1,frame2),Th]}/mean{subtract[max(frame1,frame2),Th]}, where subtract, difference, and max are operators in ImageJ's Image Calculator function and mean is the resulting image's mean pixel intensity. Th (threshold) is a constant that reduces the effects of image noise and spurious intensity fluctuations (1/8 of maximum pixel intensity by default).

To visualize the location and magnitude of the changes in cell position and area over time, the motility indexes calculated from each two consecutive frames from a time-lapse series were overlaid to generate a motility map. The dynamic range of MI scale was converted from 0 to 1 to 0 to 255.

Measurement of PLEKHG2 activity by SRE-dependent reporter assays. HEK293A cells seeded in 12-well plates were transfected with PLEKHG2 or its truncation mutants together with the pSRE-luciferase reporter plasmid and the pMAX GFP vector, in the presence or absence of Gβ1γ2 or Gβ1 point mutants and γ2. Four hours posttransfection, cells were serum starved overnight, washed twice with saline, and then lysed with lysis buffer (100 mM potassium phosphate, pH 7.8, 0.2% Triton X-100). Luciferase activity was determined using 200 μM luciferin as a substrate, as described previously (24). The activity of the reporter and the fluorescence intensity of GFP were measured using the Biotek Synergy 4 microplate reader. Luciferase activity was normalized against GFP intensity.

To assess LPA-stimulated PLEKHG2 activity, HEK293A cells were cotransfected with 25 ng of PLEKHG2 in the presence or absence of Gαt or the C terminus of G protein-coupled receptor kinase 2 (GRK2ct), pSRE-luciferase, and pMAX GFP. For the analysis of the effect of Gαt or GRK2ct, cells were transfected for 4 h, then incubated in serum-free media overnight in the presence or absence of 10 μM LPA. For PTx studies, cells were transfected for 4 h, then treated with 0.2 μg/ml PTx for 2 h, followed by stimulation with 10 μM LPA overnight. Alternatively, 4 h posttransfection, cells were incubated overnight in 1% FCS in the presence or absence of 0.2 μg/ml PTx. The following day, media were supplemented with 10 μM LPA, and cells were incubated overnight. Cells were lysed as described above, and luciferase activity was determined.

To determine the effect of the PLEKHG2 N- and C-terminal domains on basal PLEKHG2 or Vav1 activity, HEK293A cells were cotransfected with 100 ng PLEKHG2 or its mutants or Vav1 and increasing amounts of PLEKHG2 mutant 965-1385 or 1-135, pSRE-luciferase, and pMAX GFP vectors overnight. Cells were serum starved for 24 h, then harvested to assess luciferase activity. To determine the role of the PLEKHG2 N- and C-terminal domains in LPA-stimulated PLEKHG2 activity, cells were transfected with 25 ng of PLEKHG2 in the presence of increasing amounts of PLEKHG2 mutant 965-1386 or 1-135, along with pSRE-luciferase and

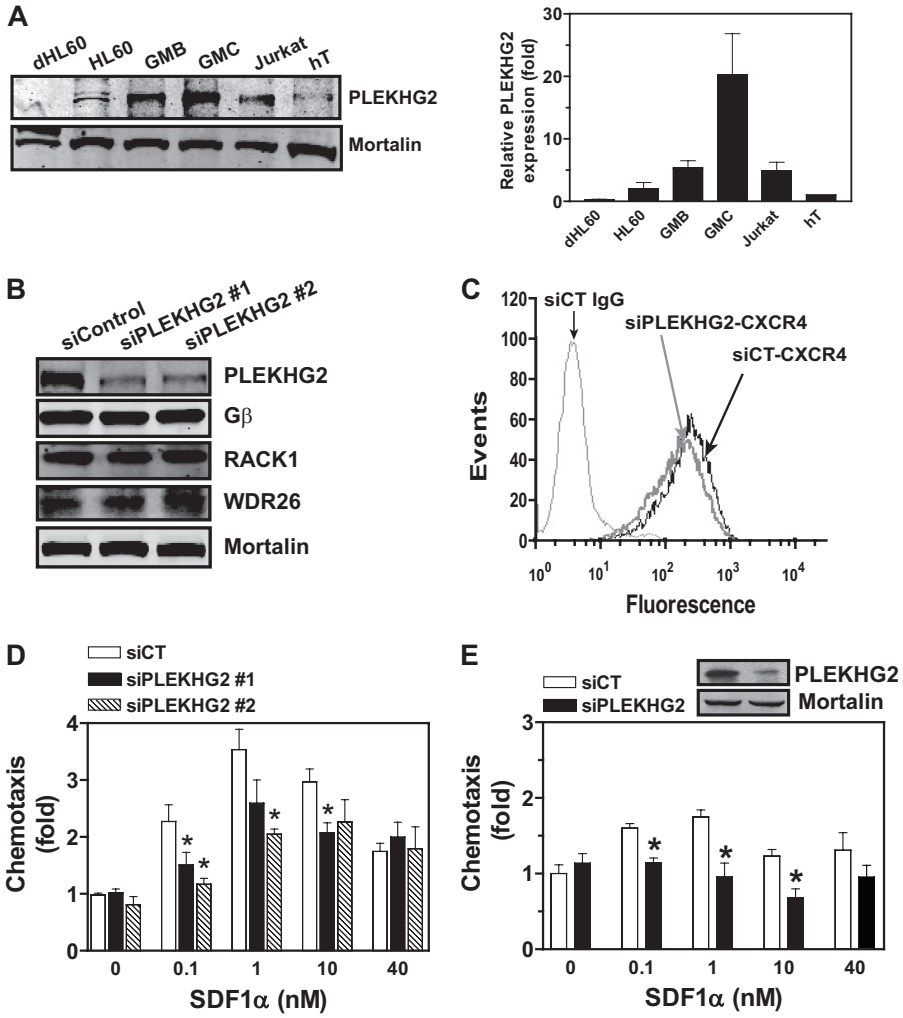

FIG 1 PLEKHG2 is required for lymphocyte migration. (A) Western blotting of PLEKHG2 expression in leukemia cell lines and human T cells. dHL60, differentiated HL60 cells; GMB and GMC, B leukemia cell lines GM18500B and GM19116C, respectively; hT, human primary T cells. PLEKHG2 expression level was quantified from 3 or 4 experiments and normalized against mortalin. Data are expressed as fold increases over the level of PLEKHG2 in human T cells. (B) Jurkat T cells transfected with a control siRNA (siCT) or PLEKHG2-targeting siRNAs (siPLEKHG2#1 and siPLEKHG2#2). Expression of PLEKHG2, Gβ, WDR26, and RACK1 was analyzed by Western blotting. (C) CXCR4 receptor expression was detected by staining transfected cells with control IgG (siCT IgG) or PE-conjugated CXCR4 antibody and was analyzed by flow cytometry. (D and E) Chemotaxis was induced in siRNA-transfected Jurkat (D) and GM18500B (E) cells by SDF1α and determined by the modified Boyden chamber assay. The chemotaxis assay was performed in triplicate and results were quantified from three to five experiments. (Top) Representative blots showing the level of PLEKHG2 in transfected GM18500B cells. *, $P < 0.05$ versus siCT.

pMAX GFP overnight. Cells were then incubated in serum-free media in the presence or absence of LPA (10 μM) and harvested for luciferase measurements after 24 h.

Data analysis. Unless indicated otherwise, data were representative of at least three independent experiments with similar results. Results are expressed as the means ± 1 standard error of the mean (SEM) from multiple experiments. Student's *t* tests were used to determine significant differences (two-tailed, $P < 0.05$).

RESULTS

PLEKHG2 is required for lymphocyte migration. As PLEKHG2 was implicated in B cell and myeloid leukemias, we first examined its expression in human primary T lymphocytes and several leukemia cell lines (7). A low level of PLEKHG2 can be detected in primary human T lymphocytes and in HL60 cells, a promyelocytic leukemia cell line. However, it was not detected in differentiated HL60 cells, which resemble human neutrophils (Fig. 1A). Interestingly, a significantly higher level of PLEKHG2 was detected in Jurkat T cells, a human T leukemia cell line, and GM19116C and GM18500B, two human B leukemia cell lines, suggesting that PLEKHG2 may be upregulated in a subset of leukemia cell lines (Fig. 1A).

To determine the potential contribution of PLEKHG2 to Gβγ-mediated leukocyte function, we initially chose Jurkat T cells as a model system, because stimulation of the endogenously expressed chemokine receptor CXCR4 results in a robust chemotactic response and Rac and Cdc42 activation through Gβγ (19, 25, 26). PLEKHG2 was knocked down in Jurkat T cells using two different siRNAs targeting unique sequences of PLEKHG2. The siRNA specifically and robustly knocked down PLEKHG2 (~70%) without affecting the expression of Gβ, CXCR4, and other Gβγ-interacting proteins, including RACK1 and WDR26 (Fig. 1B and C). Moreover, the levels of mRNA of other RhoGEFs in Jurkat T cells,

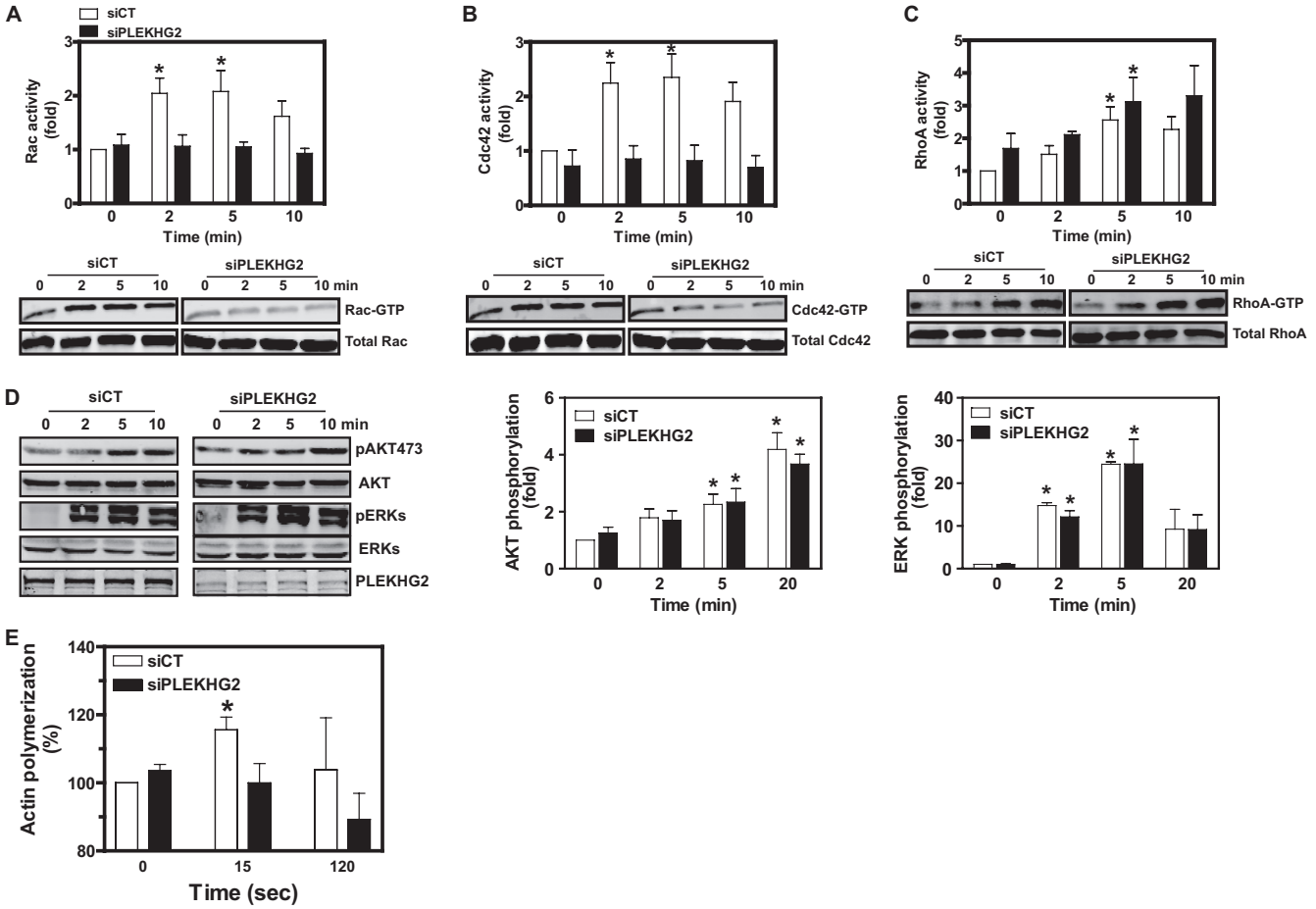

FIG 2 PLEKHG2 is required for SDF1α-mediated Rac and Cdc42, but not RhoA, activation in Jurkat cells. Jurkat T cells transfected with a control or PLEKHG2 siRNA were serum starved, then stimulated with SDF1α (50 nM). (A to C) Active Rac (A), Cdc42 (B), and RhoA (C) were pulled down using GST-PAK and GST-RBD conjugated to glutathione beads and detected by Western blotting. The presence of total Rac1, Cdc42, or RhoA in the lysates (5%) was also examined. (D) AKT and ERK phosphorylation determined by Western blotting. Quantification of Western blotting results was performed by densitometry analysis of 3 to 5 experiments. (E) Actin polymerization. Following SDF1α stimulation, F-actin was isolated from the transfected Jurkat T cells, stained with Alexa Fluor 488-conjugated phalloidin, and quantified by measuring fluorescence intensity using a microplate reader. Data are expressed as fold changes over (A to D) or percentages of (E) siCT at 0 min. *, $P < 0.05$ versus siCT at 0 min.

including Vav1/2, ARHGEF5, and DOCK2, were not significantly affected by knockdown of PLEKHG2 (data not shown). As expected, SDF1α stimulated Jurkat T cell migration in a dose-dependent manner, as assessed by Transwell assay (Fig. 1D). Downregulation of PLEKHG2 significantly inhibited Jurkat T cell migration in response to SDF1α (Fig. 1D). SDF1α also stimulated chemotaxis of GM18500B cells, although their response to SDF1α stimulation was not as robust as that of Jurkat T cells, likely due to their lower level of CXCR4 expression (data not shown). Downregulation of PLEKHG2 similarly abolished GM18500B cell migration by SDF1α stimulation (Fig. 1E). Together, these data indicate that PLEKHG2 is required for migration in a subset of leukemia cells.

PLEKHG2 mediates Jurkat T cell migration via activation of Rac and Cdc42 to facilitate actin polymerization. To identify the mechanism by which PLEKHG2 regulates migration, we first determined which Rho GTPases were regulated by PLEKHG2 in Jurkat T cells. We performed a pulldown of active Rac, Cdc42, and RhoA in Jurkat T cells transfected with a control or PLEKHG2-targeting siRNA. PLEKHG2 knockdown inhibited SDF1α-stimulated Rac and Cdc42, but not RhoA, activation (Fig. 2A, B, and C). Moreover, suppression of PLEKHG2 had no effect on the activation of other Gβγ effectors, including AKT and ERK phosphorylation (Fig. 2D). These findings indicate that PLEKHG2 specifically activates Rac and Cdc42 in Jurkat T cells.

As activation of Rho GTPases promotes actin cytoskeletal rearrangement, we assessed whether knockdown of PLEKHG2 inhibited actin polymerization (1). As reported previously, stimulation of Jurkat T cells with SDF1α resulted in a transient increase in actin polymerization (Fig. 2E) (25, 26). Suppression of PLEKHG2 alleviated actin polymerization stimulated by SDF1α.

To determine how Gβγ-mediated PLEKHG2 activation promotes Rac and Cdc42 activation and actin polymerization, we investigated the dynamics of Rac and Cdc42 activation and actin polymerization by live-cell imaging of Jurkat T cells transiently expressing the fluorescence-based probes PAK-PBD-YFP and Lifeact-RFP. The Lifeact-RFP probe binds specifically to filamentous actin (F-actin) and was used to analyze actin polymerization (27). PAK-PBD-YFP was used to probe for Rac and Cdc42 activation, as the PAK-PBD domain binds both active Rac and Cdc42 *in*

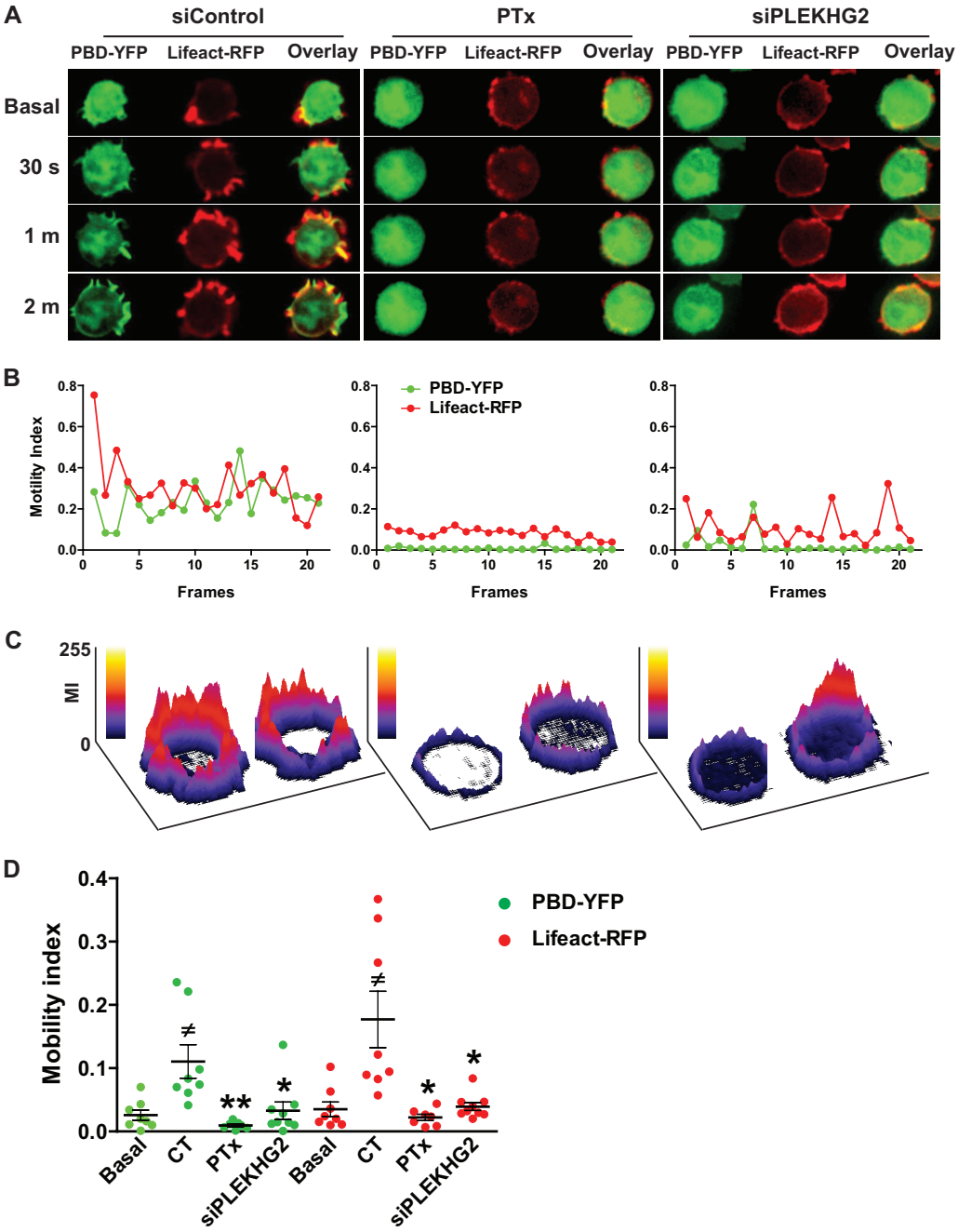

FIG 3 PLEKHG2 is required for SDF1α-mediated Rac and Cdc42 membrane translocation and actin protrusion formation. (A) Jurkat T cells were transiently transfected with a control (siControl) or PLEKHG2 (siPLEKHG2) siRNA. After 48 h, cells were transfected with Lifeact-RFP and PBD-YFP and treated or not treated with pertussis toxin (PTx) overnight. After serum starvation, basal and SDF1α-simulated PBD-YFP and Lifeact-RFP dynamics were monitored by time-lapse imaging. Images are representative of multiple cells from at least 3 experiments. (B) Motility index calculated from frames 4 to 25 (−15 s to 5 min) in the image series of a representative cell in panel A as described in Materials and Methods. (C) Heat maps showing dynamic motility changes (frames 4 to 25) of PBD-YFP and Lifeact-RFP in representative cells from panel A over time. Color indicators of the motility index (MI) range (0 to 255) are shown. (D) Average motility indexes of multiple cells unstimulated (basal) or stimulated with SDF1α (CT, PTx, and siPLEKHG2) from 3 or 4 experiments. ≠, $P < 0.05$ versus basal; * and **, $P < 0.05$ and $P < 0.01$, respectively, versus siControl PBD-YFP or Lifeact-RFP.

vitro (28, 29). To exclude the potential inhibitory effects of overexpressing PAK-PBD-YFP and Lifeact-RFP, we chose cells expressing modest levels of PAK-PBD-YFP and Lifeact-RFP for real-time imaging. As shown in Fig. 3A and in Video S1A in the supplemental material, the resting cells appeared rounded, and PAK-PBD-YFP was distributed primarily in the cytosol, whereas Lifeact-RFP was localized predominantly to the cortical membranes of these cells. Upon stimulation with a uniform concentration of SDF1α, PAK-PBD-YFP was rapidly translocated from the cytosol to the plasma membrane and the cells generated multiple

protrusions enriched with PAK-PBD-YFP and Lifeact-RFP around the cell periphery. PAK-PBD-YFP largely colocalized with Lifeact-RFP in the SDF1α-stimulated cells. To quantify the dynamics of Rac and Cdc42 activation and actin polymerization in the SDF1α-stimulated cells, a motility score (MI) was calculated as the mean difference of pixel-by-pixel change in fluorescence area between two successive frames of the image series (range, 0 to 1) in each cell (30). This MI analysis determines, in an unbiased manner, the dynamic changes in cell shapes and position from frame to frame in a time-lapse series. As shown from Video S1A in the supplemental material, Jurkat T cells did not undergo significant relocation by stimulation with a uniform concentration of SDF1α. The most obvious changes to cell morphology following SDF1α stimulation were the formation of distinct protrusions enriched with PBD-YFP and Lifeact-RFP. Therefore, the motility index analysis essentially quantified the dynamic changes from frame to frame in the formation of protrusions enriched with PBD-YFP and Lifeact-RFP. As shown in Fig. 3B and D, following SDF1α stimulation of cells transfected with a control siRNA, the motility scores of PAK-PBD-YFP and Lifeact-RFP were significantly increased compared to those for unstimulated cells and the probes exhibited similar dynamic changes. Moreover, further analysis of the location and magnitude of the MIs from each probe in a motility map indicates that the change in dynamics of both probes occurred primarily near the cell surface (Fig. 3C). These findings indicate that activation of Rac/Cdc42 at the membrane by Gβγ is correlated with actin polymerization. In support of this notion, pretreatment of cells with PTx to block Gβγ activation simultaneously inhibited PAK-PBD-YFP- and Lifeact-RFP-enriched membrane protrusions (Fig. 3; see Video S1B in the supplemental material). Suppressing PLEKHG2 had a similar inhibitory effect (Fig. 3; see Video S1C), although the extent of the inhibition may be less than that of PTx treatment (Fig. 3D). To determine the specificity of PTx treatment and PLEKHG2 knockdown, we stimulated cells with OKT3, a T cell receptor (TCR) agonist. As shown in Video S2A in the supplemental material, OKT3 stimulated membrane translocation and accumulation of PBD-YFP, together with Lifeact-RFP, to one end of cells in 70 to 80% of cells examined (9 out of 12 cells). Pretreatment with pertussis toxin (data not shown) or PLEKHG2 knockdown had no effect on these responses (see Video S2B), suggesting that PLEKHG2 functions specifically downstream of Gβγ in Jurkat T cells. Together, these findings indicate that PLEKHG2 mediates Gβγ-stimulated Rac and Cdc42 activation for actin polymerization.

PLEKHG2 interacts with endogenous Gβγ. Previous work has shown that PLEKHG2 can interact with Gβ in a heterologous expression system. To determine if PLEKHG2 is activated by interaction with Gβγ, we first sought to determine whether PLEKHG2 can endogenously interact with Gβγ. As there are no antibodies currently available on the market that can be used for immunoprecipitation of endogenous PLEKHG2, we transiently transfected Jurkat T cells with FLAG-tagged PLEKHG2 and performed coimmunoprecipitation studies. In unstimulated cells, there was little association of endogenous Gβγ with PLEKHG2, as the amount of Gβγ detected in the PLEKHG2 precipitate was not significantly different from that in the IgG control (Fig. 4A). However, 15 min of stimulation with SDF1α significantly enhanced the association between endogenous Gβγ and PLEKHG2 (Fig. 4A). In contrast, Gαi subunits were not detected in the PLEKHG2 precipitates from cells with or without SDF1α stimulation (Fig. 4A). Interaction of PLEKHG2 with endogenous Gβγ was also detected in HEK293 cells (Fig. 4B). Significant interaction between PLEKHG2 and endogenous Gβγ was detected in unstimulated HEK293 cells. However, the interaction was significantly enhanced 2- to 3-fold following 5 to 15 min of stimulation with LPA, as quantified by densitometry (Fig. 4B). Similarly, no Gα subunits, including Gαs, Gαi, Gαq/11, and Gα12, were detected in the PLEKHG2 precipitates (Fig. 4B). Together, these findings indicate that PLEKHG2 selectively interacts with Gβγ released from activated Gi/o proteins by stimulation of multiple GPCRs.

To assess whether the interaction with Gβγ mediates PLEKHG2 activation, we used a luciferase reporter assay in HEK293 cells. The luciferase gene was under the control of the SRE promoter, whose transcription activity is known to be regulated by Rho GTPases (31). Under our assay conditions, coexpression with PLEKHG2 alone induced about a 2-fold increase in the luciferase reporter activity (Fig. 4C). LPA stimulation of HEK293 cells expressing the luciferase reporter, either alone or with PLEKHG2, significantly enhanced luciferase activity (~4- and 17-fold, respectively), compared to activity in untreated cells expressing luciferase alone (Fig. 4C). Cotransfection of PLEKHG2 with the Gβγ-sequestering protein Gαt or GRK2ct blocked both basal and LPA-stimulated PLEKHG2 activity (Fig. 4C), indicating that GPCR-stimulated PLEKHG2 activation is mediated by Gβγ. LPA-stimulated PLEKHG2 activity was partially blocked (~60%) by pretreatment of cells with PTx for 2 h before the addition of LPA but was completely abolished when cells were pretreated with PTx for 24 h (Fig. 4C and D). Since PTx treatment did not alter PLEKHG2 expression (Fig. 4D), these findings indicate that LPA stimulates PLEKHG2 primarily through Gβγ released from Gi/o proteins. Interestingly, under either condition, basal PLEKHG2 activation was not affected by PTx pretreatment, suggesting that it is mediated by Gβγ released from PTx-insensitive G proteins (Fig. 4C and D).

Activation of PLEKHG2 involves multiple residues located on the Gα contact surface of Gβ1. The fact that PLEKHG2 activation is blocked by Gαt suggests that the residues located on the Gα contact surface of Gβγ are involved in PLEKHG2 activation. To identify these residues, we evaluated a series of point mutants of Gβ1 at the Gα interface for their ability to stimulate PLEKHG2 when they are coexpressed with Gγ2. As shown in Fig. 5A, all Gβ1 mutants were expressed at levels similar to the wild-type level, although their protein sizes were slightly larger, likely due to the attachment of three FLAG tags instead of the one FLAG tag attached to wild-type Gβ1. Except for the mutation at residue M101, all of the Gβ point mutants tested showed a significantly decreased ability to stimulate PLEKHG2-induced luciferase expression to various extents (20 to 80%) compared to the wild-type Gβ1. The mutant residues are located all over the surface of seven β-propeller blades of Gβ1 (Fig. 5B). However, three of these residues (D228, N230, and D246) are clustered on the fifth blade, and their mutations produced the largest decrease in activity (70 to 85%). Together, these results suggest that activation of PLEKHG2 involves multiple residues located on the Gα binding interface of Gβγ.

PLEKHG2 is autoinhibited by its C terminus. We next assessed the mechanism by which Gβγ mediates PLEKHG2 activation. Previous reports suggest that PLEKHG2 binds Gβγ through the N-terminal residues 1 to 135 and that its activity is autoinhib-

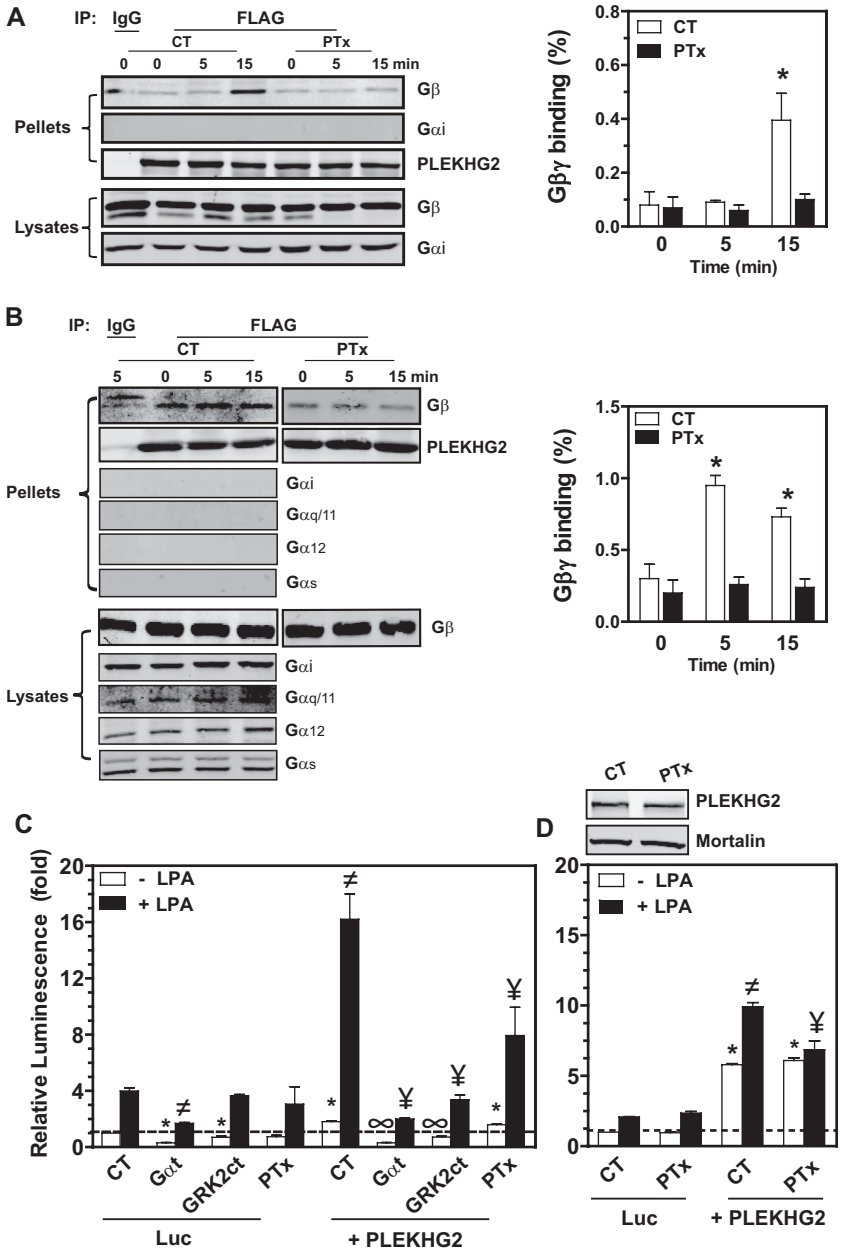

FIG 4 PLEKHG2 interaction with and activation by endogenous Gβγ. (A and B) FLAG-PLEKHG2 was immunoprecipitated from Jurkat T cells (A) or HEK293FT cells (B) pretreated with pertussis toxin (PTx) or not pretreated (CT) and stimulated with SDF1α (50 nM) (A) or LPA (10 μM) (B). Immunoprecipitation was performed with mouse IgG or anti-FLAG antibody. Immunoprecipitates (pellets) and lysates (5% of total) were probed for the indicated proteins using specific antibodies. Representative images are shown on the left, and quantitative data from 3 to 5 independent experiments are shown on the right. The amount of Gβγ-binding to PLEKHG2 is expressed as a percentage of total Gβγ in the lysates. *, $P < 0.05$ versus data at 0 min. (C and D) HEK293A cells were cotransfected with SRE-luciferase, pMAX GFP, and PLEKHG2, together with pcDNA3.1 (control), Gαt, or GRK2ct, as indicated. Cells were treated with PTx for 2 h (C) or 24 h (D) or not treated and then stimulated with LPA (10 μM) overnight. Luciferase activity was determined and expressed as fold increase over SRE-luciferase alone (Luc CT). *, ≠, ∞, and ¥, $P < 0.05$ versus Luc CT without LPA, Luc CT plus LPA, PLEKHG2 CT without LPA, and PLEKHG2 CT plus LPA, respectively ($n = 3$ or 4).

ited by its C terminus, as serial deletion of the C terminus increased its basal activity (8). To provide further evidence to support this hypothesis, we created a series of truncation mutants by deleting either the C terminus (amino acids [aa] 1 to 964 or 1 to 464), as described by Ueda et al. (8), or the N terminus (aa 104 to 1386) and then assessed their basal and Gβγ-stimulated activities (Fig. 6A).

As shown in Fig. 6B and C and consistent with data reported by Ueda et al., the C-terminal deletion mutants of PLEKHG2, 1-464 and 1-964, exhibited enhanced basal activity in an expression level-dependent manner compared to the full-length PLEKHG2. Coexpression with Gβγ resulted in further stimulation of their activities to levels higher than that of Gβγ-stimulated full-length PLEKHG2 (Fig. 6D). In contrast, the mutant with deletion of the

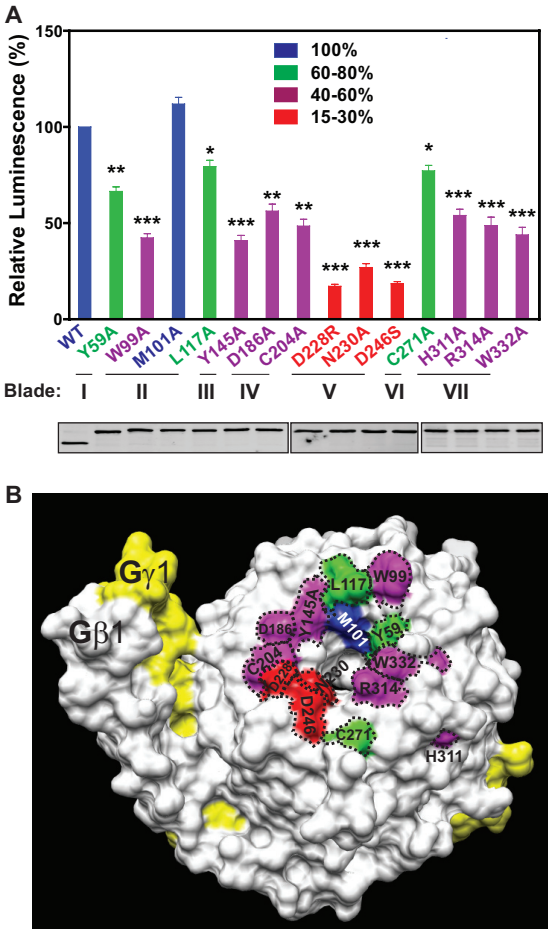

FIG 5 The effect of Gβ1 point mutation on PLEKHG2 activation. (A) HEK293 cells were cotransfected with SRE-luciferase, PLEKHG2, Gγ2, and 1×FLAG–wild-type Gβ1 (WT) or the indicated 3×FLAG-Gβ1 point mutants. Luciferase activity was determined and expressed as a percentage of WT. *, $P < 0.05$; **, $P < 0.01$; ***, $P < 0.001$ versus WT ($n = 3$ or 4). The extent of decrease in activating PLEKHG2 by Gβ1 mutants is represented by different colors. The locations of the mutant residues in the seven blades of Gβ1 are indicated below the graph. Representative blots of WT and mutant Gβ1 expression detected by an anti-FLAG antibody are also shown. (B) Locations of the mutant residues on the surface of Gβ1γ1. The mutant residues shown in panel A were mapped to the molecular surface of Gβ1γ1 generated from the crystal coordinate of Gβ1γ1 (47).

N-terminal Gβγ binding domain (104-1386) displayed a slightly decreased basal activity and lost response to Gβγ stimulation (Fig. 6B, C, and D). These findings suggest that the binding of Gβγ to the N terminus of PLEKHG2 is critical for Gβγ-mediated activation and that the C terminus of PLEKHG2 may interact with a domain beyond the N-terminal Gβγ-binding site to mediate autoinhibition.

To identify the binding sites of the C terminus on PLEKHG2, we generated an SBP-FLAG-tagged C-terminal PLEKHG2 mutant, SBP-FLAG–965-1386, and cotransfected it with myc-tagged full-length PLEKHG2 or a series of PLEKHG2 mutants, 1-964, 104-1386, 1-135, 1-464, 104-464, 104-310, and 465-964 (Fig. 7A). As a control, SBP-FLAG-tagged GFP was used. Precipitation of SBP-FLAG–965-1386 with streptavidin-conjugated magnetic beads indicates that the C terminus bound to a region consisting of at least two distinct domains, the DH domain and a domain consisting of amino acid residues 465 to 964. This binding was specific, as SBP-FLAG-tagged GFP did not interact with these domains. The DH and PH domains together (aa 104 to 464) appeared to bind the C terminus better than the DH domain alone, suggesting that the PH domain may contribute to the interaction. However, the PH domain was not expressed in these cells, so we were unable to assess its direct interaction with the C terminus.

To provide direct evidence that the PLEKHG2 C terminus inhibits PLEKHG2 activity, we cotransfected HEK293 cells with the PLEKHG2 C-terminal mutant 965-1386 (0.4 to 1.6 μg) together with the full-length protein and mutants 1-464 and 1-964 (100 ng). As shown in Fig. 8A, coexpression of the mutant 965-1386 partially (20 to 40%) inhibited the basal activity of the full-length protein and mutants 1-464 and 1-964 in a dose-dependent manner. At its highest level of expression, the mutant 965-1386 was expressed at about a 2-fold-higher level than the full-length and mutant PLKEHG2. The inhibitory effect of mutant 965-1386 is likely to be specific, as expression of the full-length or mutant PLEKHG2 was not affected and the mutant did not affect Vav1-induced luciferase reporter expression (data not shown). Moreover, the N-terminal Gβγ-binding fragment (aa 1 to 135) did not suppress the basal activity of mutant 1-464 (Fig. 8B). Rather, the highest concentration of the N-terminal mutant enhanced the basal activity of the 1-464 mutant (Fig. 8B). Notably, when the PLEKHG2 C terminus (aa 965 to 1386; 0.4 to 1.6 μg) was coexpressed with 25 ng of the full-length PLEKHG2, its basal and LPA-stimulated activities were largely abolished (Fig. 8C). Overexpression of the N terminus (aa 1 to 135; 0.4 to 1.6 μg) had a similar effect, although the extent of the inhibition was smaller (Fig. 8C). Taken together, these data indicate that the C terminus of PLEKHG2 exerts an autoinhibition on PLEKHG2 activity through interaction with the N-terminal region containing the DH domain and that Gβγ likely activates PLEKHG2, at least in part, by binding to the N terminus to relieve the autoinhibition imposed by the C terminus.

Roles of the N- and C-terminal fragments of PLEKHG2 in Jurkat T cell migration. To test whether Gβγ-binding and the release of C-terminal autoinhibition were required for PLEKHG2 activation in Jurkat T cells, we overexpressed mCherry or the mCherry-tagged PLEKHG2 N terminus (aa 1 to 135; mCherry–1-135) or C terminus (aa 965 to 1386; mCherry–965-1386) with PAK-PBD-YFP in Jurkat T cells and performed live-cell imaging. As shown in Fig. 9A, mCherry–1-135 and mCherry–965-1386 had different cellular distributions in cells. Whereas the 1-135 mutant was expressed throughout the cells, including the nucleus, cytosol, and membrane, the 965-1386 mutant was expressed primarily in the cytosol and membrane (Fig. 9A). However, overexpression of these two mutants equally blocked the translocation of PAK-PBD-YFP to the membrane protrusions stimulated by SDF1α, suggesting that these two mutants perturb Gβγ-stimulated PLEKHG2 and Rac/Cdc42 activation (Fig. 9A and B; see Video S3 in the supplemental material). Importantly, expression of the PLEKHG2 N and C termini had no effect on OKT3-stimulated PAK-PBD-YFP membrane accumulation (see Video S4 in the supplemental material), suggesting that the N and C termini specifically block Rho GTPase activation downstream of GPCRs such as CXCR4. Notably, Jurkat T cells expressing the N- and C-terminal fragments exhibited significantly decreased chemotactic responses to SDF1α stimulation, compared to control cells expressing mCherry (Fig. 9C).

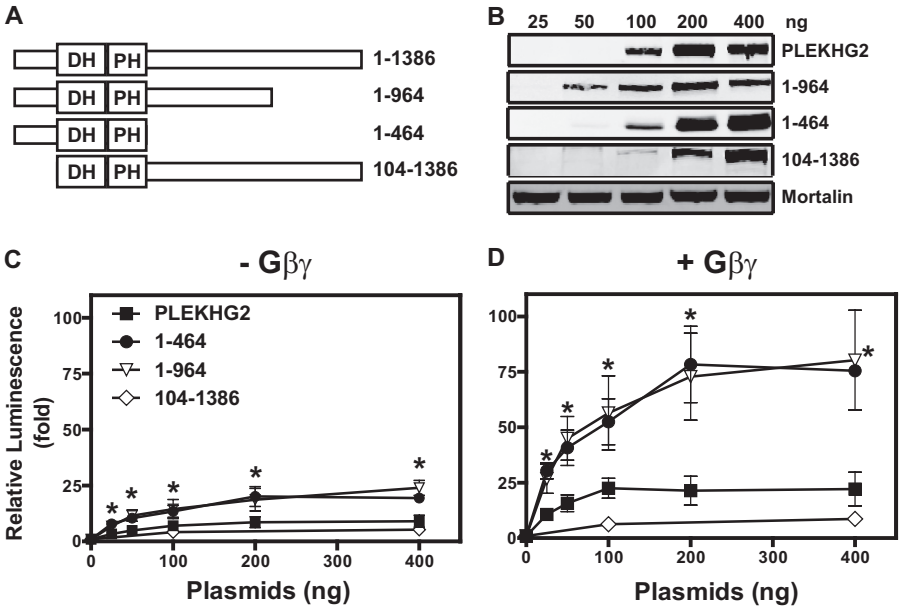

FIG 6 The contribution of PLEKHG2 N and C termini to its activity. (A) Schematic of PLEKHG2 truncation mutants. (B to D) FLAG-tagged PLEKHG2 and mutants were transiently transfected in HEK293A cells with SRE-luciferase and pMAX GFP in the presence or absence of Gβγ. (B) Level of protein expression. (C and D) Luciferase activity induced by PLEKHG2 or the truncation mutants in the absence (C) or presence (D) of Gβγ is expressed as fold change over SRE-luciferase alone. ∗, $P < 0.05$ versus PLEKHG2 alone ($n = 3$ to 5).

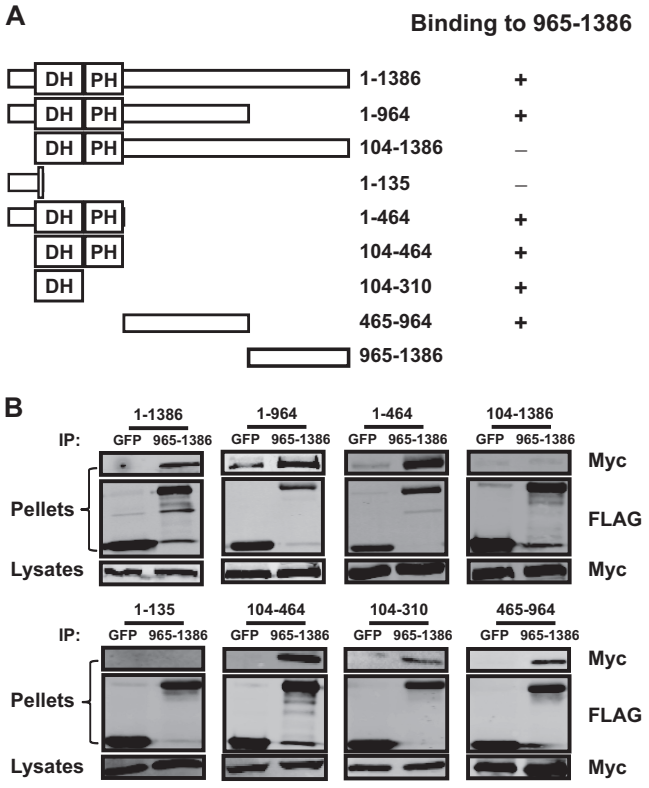

FIG 7 The binding sites of the PLEKHG2 C terminus on PLEKHG2. (A) Schematic of PLEKHG2 truncation mutants. + and − indicate binding or no binding, respectively, to the C-terminal fragment. (B) Coimmunoprecipitation (IP) of SBP-Flag-GFP or SBP-FLAG–965-1386 with myc-tagged PLEKHG2 truncation mutants in HEK293A cells. Representative blots of at least 3 experiments are shown.

DISCUSSION

Although PLEKHG2 was identified as a RhoGEF overexpressed in murine models of leukemia, the physiological and pathological roles for this protein in humans have remained unclear. In this study, we provide the first evidence for a role for PLEKHG2 in mediating chemotaxis in several human leukemia cell lines. Our data indicate that PLEKHG2 may function as a key RhoGEF that regulates lymphocyte chemotaxis through Gβγ-mediated Rac and Cdc42 activation and actin polymerization. Moreover, we have provided the molecular basis for the regulation of PLEKHG2 activity by Gβγ binding and intramolecular interactions.

The role of PLEKHG2 in mediating lymphocyte migration was demonstrated by the findings that downregulation of PLEKHG2 decreased SDF1α-induced chemotaxis in two different leukemia cell lines, Jurkat T and GM18500B cells, that overexpress PLEKHG2. PLEKHG2 appears to function specifically through the regulation of Rac and Cdc42 activation and actin cytoskeletal reorganization, because inhibition of PLEKHG2 abolishes SDF1α-stimulated Rac and Cdc42 activation and actin polymerization, but not RhoA activation and AKT and ERK phosphorylation in Jurkat T cells. The role of PLEKHG2 in regulating Rac and Cdc42 activation and actin polymerization was also demonstrated by the live-cell imaging analysis using specific probes PBD-YFP and Lifeact-RFP. It should be noted that, although the PAK-PBD domain can bind both activated Rac and Cdc42 *in vitro*, the PBD-YFP probe has been shown to primarily detect the localization of active Rac in neutrophils (28, 29). However, the selectivity of PBD-YFP for active Rac and Cdc42 in other cell types remains to be determined. Nevertheless, our findings that PLEKHG2 activates Rac and Cdc42 are consistent with a previous report in a heterologous expression system (8). Rac and Cdc42 have been shown to regulate the formation of morphologically distinct actin-rich protrusions at the plasma membranes, i.e., lamellipodia

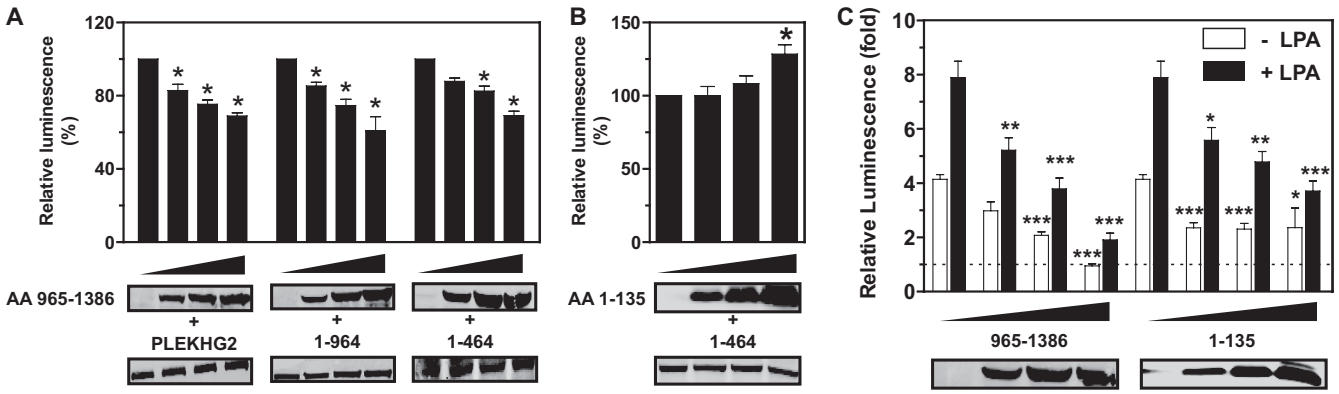

FIG 8 PLEKHG2 activation requires Gβγ binding to the N terminus and release of C-terminal autoinhibition. (A and B) FLAG-tagged PLEKHG2, 1-464, or 1-964 was coexpressed with SRE-luciferase, pMAX GFP, and increasing amounts of FLAG-tagged PLEKHG2, mutant 965-1386 (A), or mutant 1-135 (B) in HEK293A cells. Luciferase activity is expressed as a percentage of that for PLEKHG2 or mutants alone. (C) HEK293A cells were transfected with FLAG-tagged PLEKHG2, SRE-luciferase, pMAX GFP, and increasing amounts of FLAG-tagged PLEKHG2 mutant 965-1386 or 1-135 and stimulated with LPA (10 μM) overnight. Luciferase activity is expressed as a fold increase over activity for SRE-luciferase alone. Below each panel are representative blots showing the expression of PLEKHG2 and its truncation mutants. *, $P < 0.05$; **, $P < 0.01$; ***, $P < 0.001$ versus PLEKHG2 or mutants alone.

and filopodia, respectively (32). However, they are both required for cell polarization during lymphocyte migration. Whereas Rac promotes the generation of an F-actin-rich pseudopod during chemotaxis, Cdc42 defines the location and maintains the stability of pseudopod formation (1, 17, 33). The fact that PLEKHG2 is required for both Rac and Cdc42 activation suggests that the profound effect of PLEKHG2 inhibition on chemotaxis may be related to its ability to regulate both Rac and Cdc42. Nevertheless, our attempts to evaluate the relative roles of Rac and Cdc42 in SDF1α-induced Jurkat T cell migration were hampered by the fact that overexpression of the dominant negative mutants of either protein induced cell death. Moreover, several reported selective inhibitors of Rac and Cdc42, such as EHT1864 and ML141, were found to nonselectively inhibit Rac, Cdc42, and RhoA activation in our studies (data not shown) (33–35).

It has been shown previously that PLEKHG2 is activated by interaction with Gβγ (8). In line with these findings, we found that PLEKHG2 interacts with endogenous Gβγ but not Gαi subunits in Jurkat T cells stimulated with SDF1α. Specific interaction of PLEKHG2 with Gβγ can be also demonstrated in HEK293 cells stimulated with LPA, suggesting that PLEKHG2 may be activated by Gβγ downstream of multiple GPCRs. The time course of Gβγ interaction with PLEKHG2 observed in the Jurkat cells was slower (within 15 min of stimulation) than that of Rac/Cdc42 activation (within 1 to 2 min of stimulation). This is likely due to sensitivity differences between the two assays. Coimmunoprecipitation assays may not be as sensitive as Rac/Cdc42 activation assays and may require a longer time of stimulation to see the difference in association between PLEKHG2 and Gβγ than is required following basal activation. Notably, although the LPA receptor is known to couple to multiple classes of G proteins, LPA-stimulated PLEKHG2 activation is sensitive to PTx treatment, suggesting that PLEKHG2 is specifically activated by Gβγ released from Gi/o proteins. Interestingly, substantial interaction of PLEKHG2 with Gβγ can be detected in unstimulated HEK293 cells but not Jurkat T cells, and this interaction appears to be insensitive to PTx treatment (Fig. 4B). Consistent with these findings, basal activation of PLEKHG2 was also observed in HEK293 cells and activation was not affected by PTx treatment. However, the basal activity of PLEKHG2 was blocked by expression of Gβγ-sequestering Gαt and GRK2ct, suggesting that the basal activation of PLEKHG2 in HEK293 cells is mediated by Gβγ released from PTx-insensitive G proteins. How these G proteins are activated in unstimulated HEK29 cells remains unknown, because HEK293 cells were grown in serum-free media under our assay conditions. One possibility is that HEK293 cells secrete factors that stimulate GPCRs coupled to PTx-insensitive G proteins in a paracrine or autocrine manner, although such factors remain to be identified.

The finding that Gβγ-mediated PLEKHG2 activation is blocked by Gα subunits suggests that, like activation of other effectors by Gβγ, activation of PLEKHG2 by Gβγ involves residues located on the Gα contact surface of Gβ (36). In support of this notion, a series of point mutations on the Gα interface of Gβ1 impaired PLEKHG2 activation by Gβγ. The effect of these mutations is likely specific, as one of the mutants, the M101A mutant, retained the same ability as the wild-type Gβ1 to activate PLEKHG2. Additionally, previous work has demonstrated that these mutants can be copurified with Gγ2 as a complex, indicating that their deficiency in activating PLEKHG2 is not due to their failure to form a Gβγ complex (37–39). Interestingly, the mutant residues are mapped to the surface of all seven blades of Gβ1, which have been shown to form a "hot spot" engaged in interaction with a subset of Gβγ effectors (37, 40). Of these residues, three (D228, N230, and D246) are clustered on the surface of blade 5 of Gβ1 and their mutations produced the largest decrease in activation of PLEKHG2, suggesting that they may be the key molecular determinants for PLEKHG2 activation. Since two of these residues are negatively charged (D228 and D246) and mutation of these residues to a positively charged (D228R) or noncharged (D246S) residue impaired PLKEHG2 activation, these results suggest that electrostatic interaction between Gβ1 and PLEKHG2 may be critical for PLEKHG2 activation. However, it remains to be determined if these residues are engaged in direct interaction with PLEKHG2, because some of these mutations may alter the local structure of the adjacent residues and indirectly impinge on the ability of Gβγ to activate PLEKHG2.

Activation of PLEKHG2 by Gβγ likely depends on Gβγ interaction with the N-terminal fragment, aa 1 to 103, because this

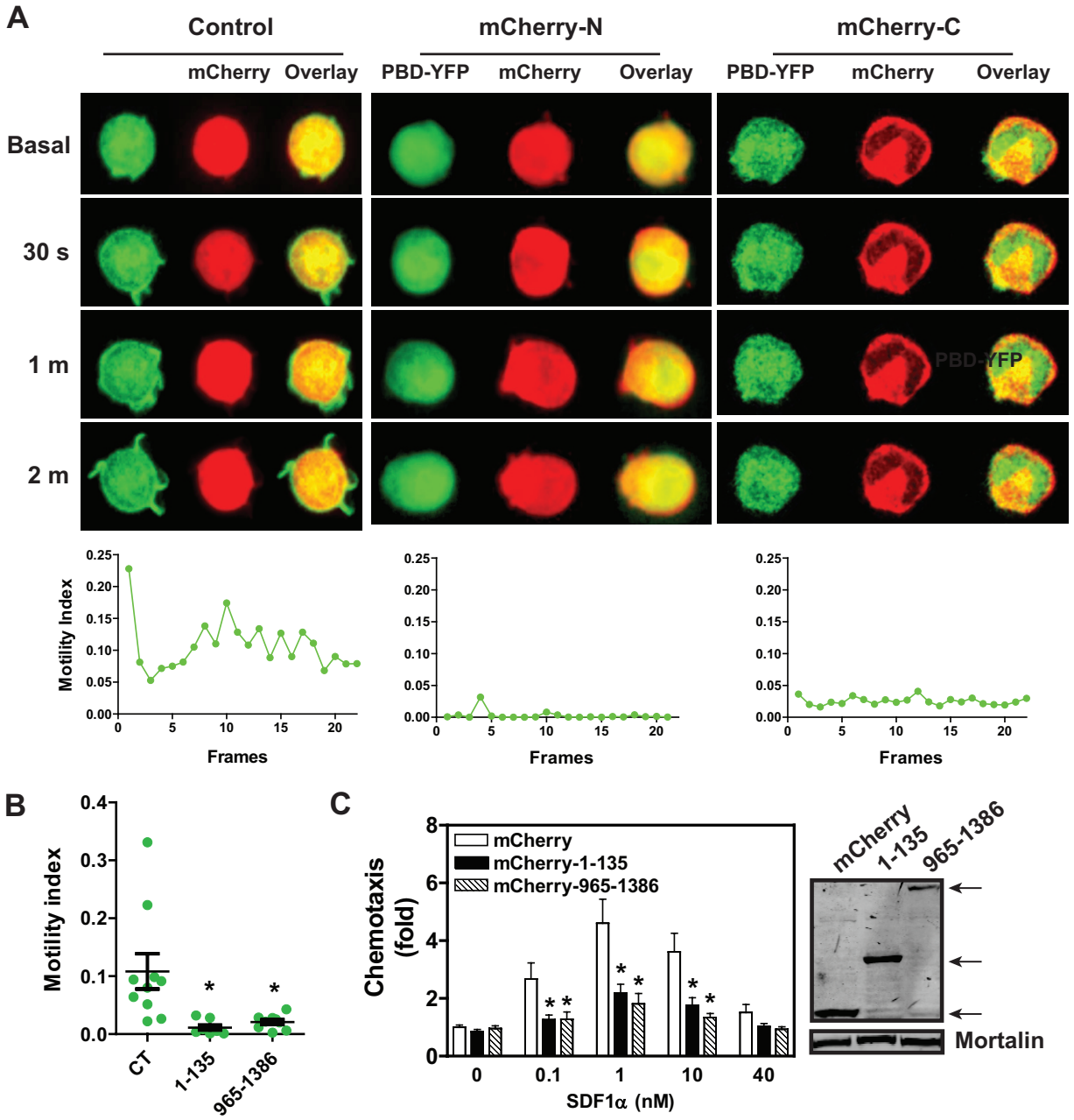

FIG 9 The contribution of PLEKHG2 N and C termini to SDF1α-induced Rac/Cdc42 activation and Jurkat cell migration. (A and B) Jurkat T cells were transfected with PBD-YFP and mCherry (control), mCherry–1-135 (mCherry-N), or mCherry–965-1386 (mCherry-C). Basal and SDF1α-stimulated PBD-YFP and Lifeact-RFP dynamics were monitored by live-cell imaging, and the motility index was calculated as described for Fig. 3. (A) Representative images and the motility index of one cell. (B) Average motility index of multiple cells. *, $P < 0.05$ versus control PBD-YFP. (C) Chemotaxis of Jurkat T cells transfected with the indicated constructs and stimulated with the indicated concentration of SDF1α. Data are expressed as fold changes over basal migration of control cells in the absence of SDF1α stimulation. (Right) Representative blots showing the expression of the indicated constructs. *, $P < 0.05$ versus mCherry control ($n = 3$).

fragment was previously shown to directly bind Gβγ, and we found that deletion of this fragment in PLEKHG2 abolishes its activation by Gβγ (8). Moreover, overexpression of the N-terminal fragment inhibits Gβγ-mediated Rac and Cdc42 activation and leukemia cell migration but has no effect on the activation of Rac and Cdc42 by the T-cell receptor agonist OKT3. Several lines of evidence indicate that, following binding, Gβγ activates PLEKHG2, at least in part, by releasing autoinhibition mediated by the C-terminal domain of PLEKHG2. First, consistent with a previous report by Ueda et al., PLEKHG2 mutants with the C-terminal domain deletion, 1-464 and 1-964, exhibit enhanced basal activity, compared to the full-length PLEKHG2 (8). These findings indicate that the C-terminal domain inhibits PLEKHG2 activity and that deletion of this domain produces PLEKHG2 constitutive activation. Second, the C-terminal domain, aa 965 to 1386, was found to bind a region encompassing the DH and PH

domains, although our coimmunoprecipitation studies could not distinguish if the interaction is mediated by direct binding of the C-terminal fragment to this region or through interaction with other proteins or lipids. Nevertheless, the interaction of the C-terminal domain with the DH domain likely prevents Rho GTPases from accessing the catalytic site of PLEKHG2. Interestingly, it has been shown recently that PLEKHG2 also interacts with the nonmuscle actin through the DH and the C-terminal domains and that the binding of actin to the DH domain attenuates PLEKHG2 activity (41). These findings indicate that, in addition to the C terminus-mediated intramolecular interaction, the activity of PLEKHG2 is also tightly regulated by other interacting proteins. Third, we have provided functional evidence that overexpression of the C-terminal fragment is sufficient to block the basal activity of full-length PLEKHG2 and the C-terminal deletion mutants of PLEKHG2. The inhibitory effect of the C-terminal fragment appears to depend on its expression level relative to that of PLEKHG2 proteins, because overexpression of the C-terminal domain at a level 2-fold higher than that of PLEKHG2 proteins caused only partial (30 to 40%) inhibition of their GEF activities. These findings suggest that, once activated, the N-terminal domain of PLEKHG2 adopts a conformation with a decreased binding affinity for the C-terminal fragment. Alternatively, the free C-terminal fragment may adopt a conformation with a reduced binding affinity for the N terminus of PLKEHG2. The ability of the C-terminal fragment to inhibit the basal activity of the full-length PLEKHG2 is consistent with our findings that, under our assay conditions, PLEKHG2 is partially activated by unknown factors through Gβγ in unstimulated HEK293 cells. The partial activation of PLEKHG2 may cause transient dissociation of the C-terminal domain from the catalytic sites, thereby allowing for competitive binding of the overexpressed C-terminal fragment. Finally, we have demonstrated that overexpression of the C-terminal fragment is sufficient to block Gβγ-mediated PLEKHG2 activation, Rac/Cdc42 activation, actin polymerization, and Jurkat T cell migration. The effect of C-terminal fragment expression is specific because it did not affect the TCR-stimulated response or the activity of another RhoGEF, Vav1. Together, our data indicate that the intramolecular interaction between the N-terminal and C-terminal domains is critical for the regulation of PLEKHG2 activity.

Although the autoinhibition imposed by the C terminus is critical for regulating PLEKHG2 activity, our data indicate that the release of this autoinhibition alone may not be sufficient for full activation of PLEKHG2. Thus, truncation of the PLEKHG2 C terminus alone did not fully activate PLKEHG2, and the activity of the truncation mutants can be further stimulated by Gβγ. These findings suggest that, in addition to releasing the inhibition mediated by the C-terminal domain, the binding of Gβγ to the N terminus may allosterically activate PLEKHG2 by inducing conformational changes in the DH and/or PH domain and/or by recruiting PLEKHG2 to the membrane, thereby promoting productive interaction of PLEKHG2 with Rho GTPases. Clearly, to further understand the molecular details of how Gβγ induces PLEKHG2 activation, future studies are required to determine the structures of various PLEKHG2 domains, either alone or in complex with Gβγ.

Several other RhoGEFs have been shown to be activated by interaction with Gβγ in leukocytes (6). These include pRex1 and ARHGEF5. pRex1 stimulates Rac and is synergistically activated by interaction with Gβγ and the phosphatidylinositol-3-kinase (PI3K) product phosphatidylinositol (3,4,5)-trisphosphate (PIP_3) (42). Activation of pRex1 may involve the direct interaction of the DH domain with Gβγ and also Gβγ- and/or PIP_3-induced membrane translocation (43, 44). pRex1 has a major function in the regulation of reactive oxygen species (ROS) production in neutrophils but plays a minor role in neutrophil chemotaxis (13, 18). ARHGEF5 is a selective RhoGEF for RhoA and related GTPases (17). It interacts with Gβγ via its PH domain and the preceding DH/PH linker region (17). It is not clear how Gβγ activates ARHGEF5, but it is presumably through the release of autoinhibition mediated by other domains in ARHGEF5, including an N-terminal helix motif and an SH3 domain at the C terminus (45, 46). ARHGEF5 is required for immature dendritic cell migration in mice during allergic airway inflammation but is dispensable for chemotaxis of other mouse leukocytes (17). Thus, PLEKHG2 may represent a novel RhoGEF that is directly activated by Gβγ and regulates both Rac and Cdc42 to promote leukocyte migration. Nevertheless, the role of PLEKHG2 in the function of normal leukocytes remains to be determined. The fact that the expression of PLEKHG2 is low in primary human T cells versus several leukemia cell lines may suggest that PLEKHG2 is not a key regulator of normal T cell chemotaxis but rather functions as an oncoprotein in leukemia cells that overexpress this protein. Given that upregulation of the mouse PLEKHG2 ortholog has been associated with mouse leukemia induced by retroviral insertion, the increased PLEKHG2 expression may contribute to the progression of leukemia, such as proliferation and dissemination of leukemia cells to various organs (7). The development of relevant mouse models of PLEKHG2 overexpression or knockout will be essential to answer these questions.

Together, our studies have identified PLEKHG2 as a novel Gβγ-stimulated RhoGEF that mediates chemokine-induced migration of several leukemia cell lines. These findings offer novel insights into the endogenous function of PLEKHG2 and support further investigation of PLEKHG2 as a potential novel oncoprotein in leukemia.

ACKNOWLEDGMENTS

We greatly appreciated Fang Lin and Stefan Strack for their assistance in the acquisition and analysis of live-cell images, respectively, Zhizeng Sun for his contribution to the identification of PLEKHG2 siRNAs, and Alan Smrcka for providing us the Gβ1 mutants.

The work was supported in part by National Institutes of Health grant GM094255 to S.C. and National Institutes of Health T32 Pharmacological science and pain training grants to C.R.

REFERENCES

1. **Sit ST, Manser E.** 2011. Rho GTPases and their role in organizing the actin cytoskeleton. J. Cell Sci. **124:**679–683.
2. **Rossman KL, Der CJ, Sondek J.** 2005. GEF means go: turning on RHO GTPases with guanine nucleotide-exchange factors. Nat. Rev. Mol. Cell Biol. **6:**167–180.
3. **Heasman SJ, Ridley AJ.** 2008. Mammalian Rho GTPases: new insights into their functions from in vivo studies. Nat. Rev. Mol. Cell Biol. **9:**690–701.
4. **Mulloy JC, Cancelas JA, Filippi MD, Kalfa TA, Guo F, Zheng Y.** 2010. Rho GTPases in hematopoiesis and hemopathies. Blood **115:**936–947.
5. **Zheng Y.** 2001. Dbl family guanine nucleotide exchange factors. Trends Biochem. Sci. **26:**724–732.
6. **Aittaleb M, Boguth CA, Tesmer JJ.** 2010. Structure and function of heterotrimeric G protein-regulated Rho guanine nucleotide exchange factors. Mol. Pharmacol. **77:**111–125.

7. **Himmel KL, Bi F, Shen H, Jenkins NA, Copeland NG, Zheng Y, Largaespada DA.** 2002. Activation of clg, a novel dbl family guanine nucleotide exchange factor gene, by proviral insertion at evi24, a common integration site in B cell and myeloid leukemias. J. Biol. Chem. **277:**13463–13472.
8. **Ueda H, Nagae R, Kozawa M, Morishita R, Kimura S, Nagase T, Ohara O, Yoshida S, Asano T.** 2008. Heterotrimeric G protein betagamma subunits stimulate FLJ00018, a guanine nucleotide exchange factor for Rac1 and Cdc42. J. Biol. Chem. **283:**1946–1953.
9. **Rickert P, Weiner OD, Wang F, Bourne HR, Servant G.** 2000. Leukocytes navigate by compass: roles of PI3Kgamma and its lipid products. Trends Cell Biol. **10:**466–473.
10. **Runne C, Chen S.** 2013. WD40-repeat proteins control the flow of Gbetagamma signaling for directional cell migration. Cell Adh. Migr. **7:**214–218.
11. **Arai H, Tsou CL, Charo IF.** 1997. Chemotaxis in a lymphocyte cell line transfected with C-C chemokine receptor 2B: evidence that directed migration is mediated by betagamma dimers released by activation of Galphai-coupled receptors. Proc. Natl. Acad. Sci. U. S. A. **94:**14495–14499.
12. **Neptune ER, Bourne HR.** 1997. Receptors induce chemotaxis by releasing the betagamma subunit of Gi, not by activating Gq or Gs. Proc. Natl. Acad. Sci. U. S. A. **94:**14489–14494.
13. **Dong X, Mo Z, Bokoch G, Guo C, Li Z, Wu D.** 2005. P-Rex1 is a primary Rac2 guanine nucleotide exchange factor in mouse neutrophils. Curr. Biol. **15:**1874–1879.
14. **Fukui Y, Hashimoto O, Sanui T, Oono T, Koga H, Abe M, Inayoshi A, Noda M, Oike M, Shirai T, Sasazuki T.** 2001. Haematopoietic cell-specific CDM family protein DOCK2 is essential for lymphocyte migration. Nature **412:**826–831.
15. **Li Z, Hannigan M, Mo Z, Liu B, Lu W, Wu Y, Smrcka AV, Wu G, Li L, Liu M, Huang CK, Wu D.** 2003. Directional sensing requires G beta gamma-mediated PAK1 and PIX alpha-dependent activation of Cdc42. Cell **114:**215–227.
16. **Nishikimi A, Fukuhara H, Su W, Hongu T, Takasuga S, Mihara H, Cao Q, Sanematsu F, Kanai M, Hasegawa H, Tanaka Y, Shibasaki M, Kanaho Y, Sasaki T, Frohman MA, Fukui Y.** 2009. Sequential regulation of DOCK2 dynamics by two phospholipids during neutrophil chemotaxis. Science **324:**384–387.
17. **Wang Z, Kumamoto Y, Wang P, Gan X, Lehmann D, Smrcka AV, Cohn L, Iwasaki A, Li L, Wu D.** 2009. Regulation of immature dendritic cell migration by RhoA guanine nucleotide exchange factor Arhgef5. J. Biol. Chem. **284:**28599–28606.
18. **Welch HC, Condliffe AM, Milne LJ, Ferguson GJ, Hill K, Webb LM, Okkenhaug K, Coadwell WJ, Andrews SR, Thelen M, Jones GE, Hawkins PT, Stephens LR.** 2005. P-Rex1 regulates neutrophil function. Curr. Biol. **15:**1867–1873.
19. **Chen S, Lin F, Shin ME, Wang F, Shen L, Hamm HE.** 2008. RACK1 regulates directional cell migration by acting on G betagamma at the interface with its effectors PLC beta and PI3K gamma. Mol. Biol. Cell **19:**3909–3922.
20. **Sun Z, Tang X, Lin F, Chen S.** 2011. The WD40 repeat protein WDR26 binds Gbetagamma and promotes Gbetagamma-dependent signal transduction and leukocyte migration. J. Biol. Chem. **286:**43902–43912.
21. **Sun Z, Runne C, Tang X, Lin F, Chen S.** 2012. The Gbeta3 splice variant associated with the C825T gene polymorphism is an unstable and functionally inactive protein. Cell Signal. **24:**2349–2359.
22. **Benard V, Bokoch GM.** 2002. Assay of Cdc42, Rac, and Rho GTPase activation by affinity methods. Methods Enzymol. **345:**349–359.
23. **Condeelis J, Hall AL.** 1991. Measurement of actin polymerization and cross-linking in agonist-stimulated cells. Methods Enzymol. **196:**486–496.
24. **Hampf M, Gossen M.** 2006. A protocol for combined Photinus and Renilla luciferase quantification compatible with protein assays. Anal. Biochem. **356:**94–99.
25. **Sotsios Y, Whittaker GC, Westwick J, Ward SG.** 1999. The CXC chemokine stromal cell-derived factor activates a Gi-coupled phosphoinositide 3-kinase in T lymphocytes. J. Immunol. **163:**5954–5963.
26. **Nishita M, Aizawa H, Mizuno K.** 2002. Stromal cell-derived factor 1alpha activates LIM kinase 1 and induces cofilin phosphorylation for T-cell chemotaxis. Mol. Cell. Biol. **22:**774–783.
27. **Riedl J, Crevenna AH, Kessenbrock K, Yu JH, Neukirchen D, Bista M, Bradke F, Jenne D, Holak TA, Werb Z, Sixt M, Wedlich-Soldner R.** 2008. Lifeact: a versatile marker to visualize F-actin. Nat. Methods **5:**605–607.
28. **Thompson G, Owen D, Chalk PA, Lowe PN.** 1998. Delineation of the Cdc42/Rac-binding domain of p21-activated kinase. Biochemistry **37:**7885–7891.
29. **Srinivasan S, Wang F, Glavas S, Ott A, Hofmann F, Aktories K, Kalman D, Bourne HR.** 2003. Rac and Cdc42 play distinct roles in regulating PI(3,4,5)P3 and polarity during neutrophil chemotaxis. J. Cell Biol. **160:**375–385.
30. **Strack S, Wilson TJ, Cribbs JT.** 2013. Cyclin-dependent kinases regulate splice-specific targeting of dynamin-related protein 1 to microtubules. J. Cell Biol. **201:**1037–1051.
31. **Hill CS, Wynne J, Treisman R.** 1995. The Rho family GTPases RhoA, Rac1, and CDC42Hs regulate transcriptional activation by SRF. Cell **81:**1159–1170.
32. **Nobes CD, Hall A.** 1995. Rho, rac, and cdc42 GTPases regulate the assembly of multimolecular focal complexes associated with actin stress fibers, lamellipodia, and filopodia. Cell **81:**53–62.
33. **Katz E, Sims AH, Sproul D, Caldwell H, Dixon MJ, Meehan RR, Harrison DJ.** 2012. Targeting of Rac GTPases blocks the spread of intact human breast cancer. Oncotarget **3:**608–619.
34. **Chen HY, Yang YM, Stevens BM, Noble M.** 2013. Inhibition of redox/Fyn/c-Cbl pathway function by Cdc42 controls tumour initiation capacity and tamoxifen sensitivity in basal-like breast cancer cells. EMBO Mol. Med. **5:**723–736.
35. **Shutes A, Onesto C, Picard V, Leblond B, Schweighoffer F, Der CJ.** 2007. Specificity and mechanism of action of EHT 1864, a novel small molecule inhibitor of Rac family small GTPases. J. Biol. Chem. **282:**35666–35678.
36. **Smrcka AV.** 2008. G protein betagamma subunits: central mediators of G protein-coupled receptor signaling. Cell. Mol. Life Sci. **65:**2191–2214.
37. **Davis TL, Bonacci TM, Sprang SR, Smrcka AV.** 2005. Structural and molecular characterization of a preferred protein interaction surface on G protein beta gamma subunits. Biochemistry **44:**10593–10604.
38. **Ford CE, Skiba NP, Bae H, Daaka Y, Reuveny E, Shekter LR, Rosal R, Weng G, Yang CS, Iyengar R, Miller RJ, Jan LY, Lefkowitz RJ, Hamm HE.** 1998. Molecular basis for interactions of G protein betagamma subunits with effectors. Science **280:**1271–1274.
39. **Yoshikawa DM, Bresciano K, Hatwar M, Smrcka AV.** 2001. Characterization of a phospholipase C beta 2-binding site near the amino-terminal coiled-coil of G protein beta gamma subunits. J. Biol. Chem. **276:**11246–11251.
40. **Scott JK, Huang SF, Gangadhar BP, Samoriski GM, Clapp P, Gross RA, Taussig R, Smrcka AV.** 2001. Evidence that a protein-protein interaction 'hot spot' on heterotrimeric G protein betagamma subunits is used for recognition of a subclass of effectors. EMBO J. **20:**767–776.
41. **Sato K, Handa H, Kimura M, Okano Y, Nagaoka H, Nagase T, Sugiyama T, Kitade Y, Ueda H.** 2013. Identification of a Rho family specific guanine nucleotide exchange factor, FLJ00018, as a novel actin-binding protein. Cell Signal. **25:**41–49.
42. **Welch HC, Coadwell WJ, Ellson CD, Ferguson GJ, Andrews SR, Erdjument-Bromage H, Tempst P, Hawkins PT, Stephens LR.** 2002. P-Rex1, a PtdIns(3,4,5)P3- and Gbetagamma-regulated guanine-nucleotide exchange factor for Rac. Cell **108:**809–821.
43. **Hill K, Krugmann S, Andrews SR, Coadwell WJ, Finan P, Welch HC, Hawkins PT, Stephens LR.** 2005. Regulation of P-Rex1 by phosphatidylinositol (3,4,5)-trisphosphate and Gbetagamma subunits. J. Biol. Chem. **280:**4166–4173.
44. **Barber MA, Donald S, Thelen S, Anderson KE, Thelen M, Welch HC.** 2007. Membrane translocation of P-Rex1 is mediated by G protein betagamma subunits and phosphoinositide 3-kinase. J. Biol. Chem. **282:**29967–29976.
45. **Yohe ME, Rossman K, Sondek J.** 2008. Role of the C-terminal SH3 domain and N-terminal tyrosine phosphorylation in regulation of Tim and related Dbl-family proteins. Biochemistry **47:**6827–6839.
46. **Yohe ME, Rossman KL, Gardner OS, Karnoub AE, Snyder JT, Gershburg S, Graves LM, Der CJ, Sondek J.** 2007. Auto-inhibition of the Dbl family protein Tim by an N-terminal helical motif. J. Biol. Chem. **282:**13813–13823.
47. **Sondek J, Bohm A, Lambright DG, Hamm HE, Sigler PB.** 1996. Crystal structure of a G-protein beta gamma dimer at 2.1A resolution. Nature **379:**369–374.